

RESEARCH ARTICLE

Using ZnO based on Bentonite as a nano photocatalyst for degradation of Acid Red 114 in synthetic wastewater

Reza Hekmatshoar¹, Ahmad Reza Yari², Aref Shokri^{3*}

¹ Department of Occupational Health & Safety Engineering, Sabzavar University of Medical Science Sabzavar, Iran.

² Department of Occupational Health & Safety Engineering, Qhom University of Medical Science Qhom, Iran.

³ Department of chemistry, Faculty of Science, Payamenoor University, Tehran, Iran.

ARTICLE INFO

Article History:

Received 2019-04-21

Accepted 2020-07-11

Published 2020-10-01

Keywords:

nano photo catalyst

Acid red 114 (AR 114)

Co-precipitation Method

Batch photo reactor

ABSTRACT

In this project, the removal of Acid Red 114 (AR 114) that is a mono Azo dye with global usage in an aqueous environment was explored by nano photocatalytic process. The ZnO was supported on Bentonite and used at suspension state in a batch photoreactor. The catalyst was synthesized by co precipitation methods and characterized by Scanning Electronic Microscopy (SEM), X-Ray Diffraction (XRD), and Fourier Transform Infrared (FT-IR) spectra. The effect of operational variables including pH, initial concentration of Acid red 114, amounts of catalysts and temperature were investigated on the removal efficiency of AR114. The optimum conditions were achieved at 1g/l of catalyst, 30 mg/l of AR 114, pH of 9 and temperature at 35°C. The removal of AR 114 in UV, UV/ZnO, and UV/ZnO/Bentonite process were 26.5, 55 and 92.5% after 2 h of treatment, respectively. The photo catalytic degradation mechanism was described and the efficiency of the process increased considerably by modification of photocatalyst.

How to cite this article

Hekmatshoar R., Yari A.R., Shokri A. Using ZnO based on Bentonite as a nano photocatalyst for degradation of Acid Red 114 in synthetic wastewater. J. Nanoanalysis., 2020; 7(4): -10. DOI: 10.22034/jna.***.

INTRODUCTION

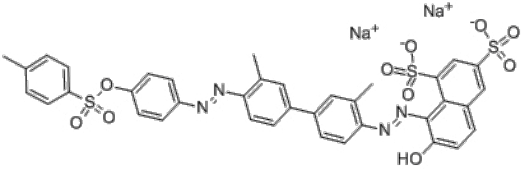
The synthetic dyes are widely used in the textile, pharmaceutical, paper, cosmetics, food, and leather industries [1-2]. Traditional colors are usually divided into a variety of acid colors, reactive and direct colors, basic, and other groups. Azo dyes are one of the largest groups of synthetic dyes that have one or more Azo bonds [3], and they are used in various types of industries due to their high solubility, low cost, stability and high color variation [4]. Therefore, due to the risks associated with the release of colored wastewater to the environment without using appropriate treatment, the treatment of this type of wastewater is necessary. Common methods such as coagulation and flocculation, biological processes, and chemical deposition are not able to treat this type of wastewater properly [5]. Biological processes do not effect on the removal of these pollutants, and classical

treatment processes not effective because they generate solid waste and transfer pollution from one phase to another. The conventional methods themselves cause environmental pollution, so the use of advanced oxidation processes (AOPs) will be essential. In these processes, active free radicals such as hydroxyl (OH[•]) are produced, which have a very high oxidizing power for the decomposition of organic pollutants due to their high oxidation potential (EOH[•] = 2.80 eV) [6]. These radicals have enough ability to react selectively with organic molecules to produce dehydrogenated or hydroxyl derivatives until they degraded completely and mineralized to CO₂, water and mineral ions [7].

Among different photo catalysts, ZnO and TiO₂ have been employed widely because of their uses in degradation of different environmental contaminants [8-10]. Zinc Oxide has single optical and electrical features with significant requests, such as solar cells apparent conducting films, photo

* Corresponding Author Email: aref.shokri3@gmail.com

Table 1. The characteristics of the used Acid Red 114.

Color name	Chemical Structure	λ_{max}	Molecular Weight(g/mol)
Acid Red 114		522	830.8

catalyst and antibacterial constituents [11-13]. So far, many researches had focused on investigation of slurry systems, in which the suspensions with powdered photo catalysts are employed [14].

The ZnO along with other modifiers had many applications. For example, Karthik et al., realized that the CdO-ZnO Nano catalyst had notable antibacterial efficiency against many microbial organisms. The hydrogen peroxide that is a microbe killer has produced at the surface of CdO-ZnO Nano catalyst, and the positive charge of Zn^{2+} and Cd^{2+} was released from catalyst to absorb the negative charge on the casing of microbial cells causing the loss of microbes [15]. The photo catalytic degradation of methylene blue by nano RGO-ZnO was investigated by Luo et al., and they found out that the efficiency was increased by 67% because the charge carrier recombination was inhibited by the interaction of ZnO with RGO [16]. Barpuzary et al. investigated the improved electron transfer with the arrangement of GO, CdS and ZnO in nano catalyst structure [17-18].

The UV/ZnO process as a photo catalyst is a branch of AOPs with low operations cost. The use of ZnO suspension can improve the decomposition efficiency of organic pollutants in wastewater. Therefore, in this study, the ZnO catalyst was modified by supporting on Bentonite through coprecipitation method and it was characterized by SEM, XRD, and FT-IR spectra test, then its efficiency was explored on the removal of AR114 in aqueous environment. The photo catalytic degradation mechanisms were described and optimum operational variables were obtained.

EXPERIMENTAL MATERIALS

In this study, the Acid Red 114 (AR114) was supplied from R.O.D. Company in China and examined without further purification. It is in the

form of a dark red powder, soluble in water, and its chemical structure is shown in Table 1. Zinc acetate, Potash, Sulfuric acid and ethanol were also purchased from Merck. Bentonite clay was used as a solid base for ZnO photo catalyst that is obtained from Kansas Jam Company, Rasht, Iran.

Photo Reactor

The batch glass reactor with 50 cm in length, 25 cm in wide and 7 cm in height were used. The air was bubbled from the bottom into the reactor through a sparger. In all experiments, the aeration rate was constant and uniform, and the magnet was placed in the middle of the reactor to stir the solution. Around the reactor was completely covered with insulation to prevent penetrating UV lights to outside. In addition, due to the high surface of the reactor and its low height, it was possible to diffuse oxygen uniformly throughout the reactor.

The conditions for all sampling were the same, and all the solutions were exposed to ultraviolet light without having a dead zone. The catalyst particles were suspended and slightly settled by stirring and aerating. The experimental set up was presented in Fig.1.

The ultraviolet light source is a UV lamp from Philips Company in Holland with a diameter of 2 cm, a length of 43 cm with a power of 15 w. This lamp is of low mercury pressure type. The radiation of this lamp covers the entire ultraviolet range, but its main wavelength range is suitable for 160-300 nm and its maximum radiation is measured at the wavelength of 522 nm. The lamp was placed horizontally above the reactor for the uniform radiation of the solution in the reactor. The distance from the lamp to the surface of the reactor solution was 20 cm. The pH was adjusted by H_2SO_4 and NaOH solution by PT-10P Sartorius pH meter.

During experiment, the temperature was

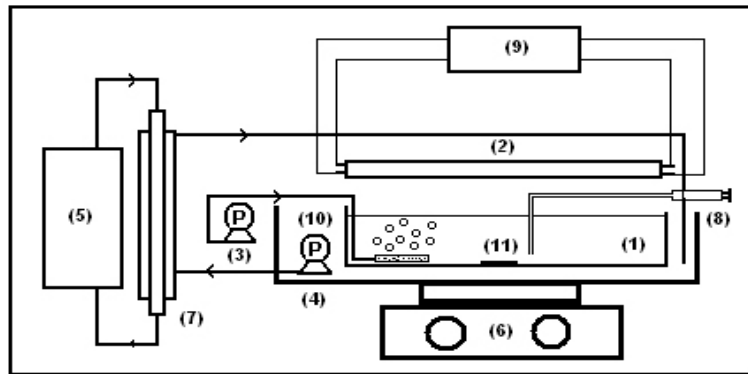


Fig. 1. Schematic diagram of photo catalytic batch reactor:(1- Effluent solution 2- UV lamp 3- Aeration pump 4- Batch reactor, 5-thermo-Bath, 6-magnetic Stirrer, 7-Heat exchanger 8-sampling Point, 9-power supply source 10-Circular pump 11- Magnetic bar).

Table 2. Summary of the stages of experiments investigating the influencing factors in degradation of AR 114.

Temperature °C	Initial concentration of AR 114	pH	Catalyst Concentration(g/l)	Irradiation W	← variable Test↓
35	30	3-11	1	15	Run1
35	30	9	0.5-2.5	15	Run2
20-35	30	9	1	15	Run3
35	20-50	9	1	15	Run4
35	30	9	1	15	Run5

regulated by thermostat, RW-0525GS model from Korea. The water flow was transferred to the thermal bath by a plastic interface pipe. Finally, the output water flow was returned to the thermostat, thus controlling the reactor temperature according to the test conditions. An aeration pump BS-310 model, with 220V and 3 W from China was used to saturate the solution with oxygen.

General procedure of experiments

In photo catalytic process, catalyst, color, temperature and pH values were determined for each experiment. At first, the UV lamp was switched off and the solution was aerated and stirred for 30 min for adsorption of the dyes, then the UV lamp was started and the reaction proceeded for 120 min. The Samples were withdrawn every 20 min and centrifuged to separate the catalyst particles. The absorption of samples was measured using Perkin-Elmer (Lambda 25) UV-VIS spectrophotometer at 522 nm. Based on Beer Lambert equation the absorption was related to the concentration and therefore, the concentration of the samples was determined.

In this study, the one factor at a time (OFAT)

method was used to optimize the process variables including pH, initial concentration of Acid red 114, amounts of catalysts and temperature. A summary of the process conditions are given in Table 2.

The concentration of AR 114 solutions was determined and the photo degradation efficiency as a function of time is given as the following (Eq. 1) :

$$AR114\ Removal(\%) = \left(\frac{[AR114]_0 - [AR114]}{[AR114]_0} \right) \times 100 \quad (1)$$

Where $[AR114]_0$ and $[AR114]$ are the concentration of AR 114 at $t=0$ and t , respectively.

In order to study the degradation of AR 114 after every 20 min of irradiation, the solution was sampled and their absorption spectrum was recorded. These spectra are given in Fig. 2. Based on these results, it was found that the structure of the AR114 molecules is broken due to ultraviolet radiation in the Batch reactor and the absorption intensity was reduced. As illustrated in Fig.2, the spectrum of AR 114 has a main peak at 520 nm and as mentioned above, its removal was calculated from the changes in this peak. It should be mentioned that the AR114, has other tow peaks at 245 and 325 nm, which are not displayed in the

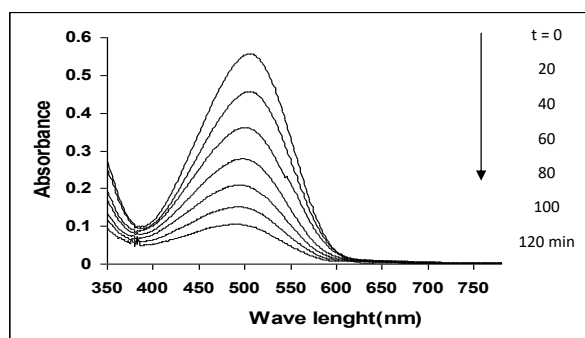


Fig .2. UV Visible spectra of AR 114 (pH at 9, Initial concentration of AR114 at 30 mg/l, temperature at 25, and 120 min of reaction).

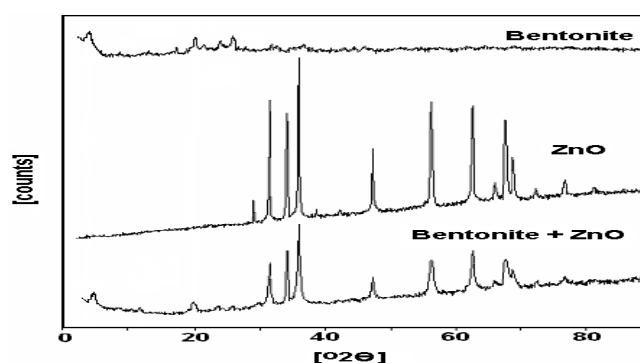


Fig. 3. XRD pattern of ZnO and ZnO/ Bentonite.

Figure. The spectral height in 518 nm was decreased rapidly which is due to the breakage of N=N bond of the dyes by hydroxyl radicals.

Preparation of ZnO supported on Bentonite

At first, a saturated solution containing 100 ml of zinc acetate, $Zn(CH_3COO)_2 \cdot 2H_2O$, was prepared by mixing with magnetic stirrer completely, then the KOH (5M) was added to the solution dropwise. After adding each drop, a jelly deposit was formed. After adding each 5 ml of KOH, a little of the solution was poured into the test tube and centrifuged at a rate of 5 rpm for ten min, then a drop of KOH was added to the solution inside the test tube and stirred a little to form $Zn(OH)_2$ deposits as the gelatinous precipitate. The addition of KOH to the formed precipitate was continued until the precipitate can be solved in the KOH and the precipitate was not formed meaning that all of the present zinc in the solution was combined with hydroxide ions to form $Zn(OH)_2$. In this situation, the addition of KOH was stopped, and then the solution was mixed uniformly for 12 hours. The resulting precipitate was filtered using filter paper

and rinsed three times with ethanol for water removal. The precipitate was placed in an oven at 110 °C for two hours to be dried and then it was placed in the oven for calcination at 450 °C for 2 hours. The XRD, FT IR and SEM techniques were used to determine the quality of the catalyst. For the preparation of ZnO based on Bentonite, about 100 ml of a saturated solution containing zinc acetate was mixed with Bentonite powder until the magnet rotates hardly, then the adding Bentonite was stopped and the procedure was continued as the previous stage with only ZnO.

RESULTS AND DISCUSSIONS

XRD analysis

The crystal structure of the samples was investigated by X-ray diffraction via Cu K α radiation ($\lambda = 0.15418$ nm). The specimens were examined in angular range at 2θ from 10 to 90 degrees. All patterns matched the standard templates.

The XRD patterns of ZnO and ZnO supported on Bentonite are showed in Fig. 3. The peaks in 2θ round at 62.89°, 56.62°, 47.57°, 36.29°, 34.46°, 31.77°, have been associated with the hexagonal

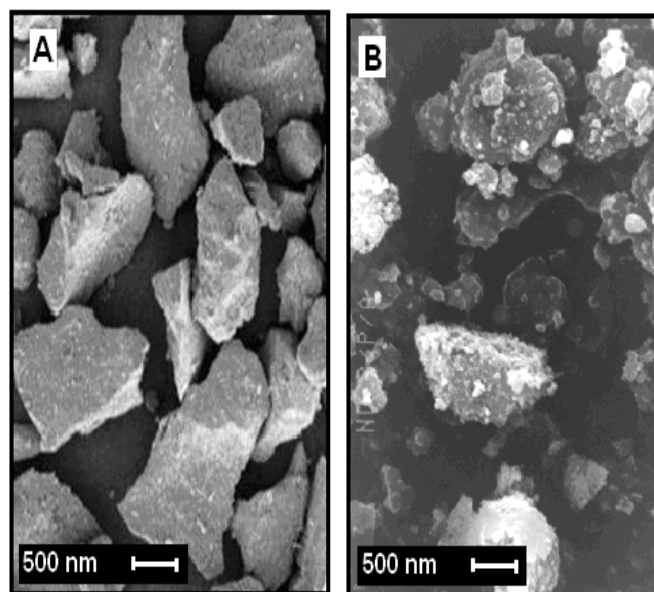


Fig. 4. SEM image of; (A) ZnO and (B) ZnO/BT.

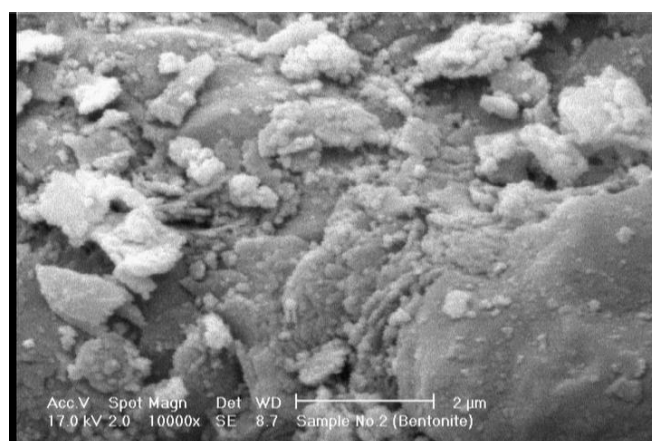


Fig. 5. SEM image of ZnO/BT.

wurtzite phase of ZnO [19]. It was clear that there is ZnO in the initial zeolite structure, so the location of the peaks was not changed considerably, so it can be concluded that the crystal structure of ZnO was not changed when supported on Bentonite. The increase in the intensity of these peaks indicates an increase in the amount of ZnO in zeolite structure. As investigated by other researchers, the ordered preparation and crystallinity of the synthesized sample can be investigated over the XRD results [20]. Additionally, the highest peaks of Bentonite at 2θ about 20° remained with a similar form showing that the structure of Bentonite is undamaged after

ZnO modification. The intensity of a little number of distinct peaks of Bentonite vanished while comparing the XRD spectrum of Bentonite and ZnO/BT, this is originated from the covering of bentonite surface by ZnO effectively.

SEM images

The SEM images of the catalyst are shown in Figs. 4 and 5. These images showed that the size of the ZnO particles is large to settle in the pores of Bentonite. According to SEM images, the dimensions of the ZnO are larger than the dimensions of the cavities in Bentonite zeolite.

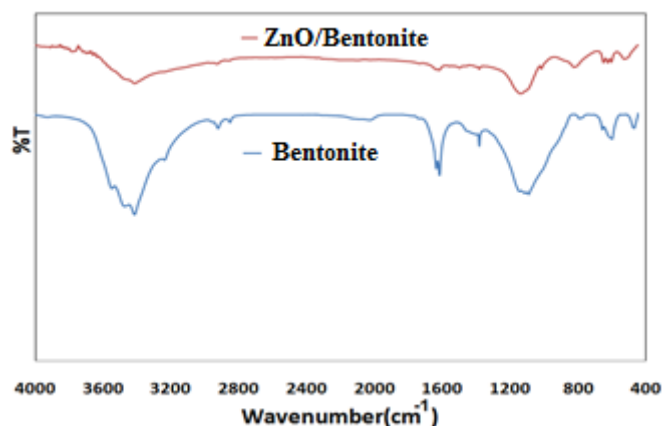


Fig. 6. FTIR spectra of the Bentonite and ZnO/Bentonite.

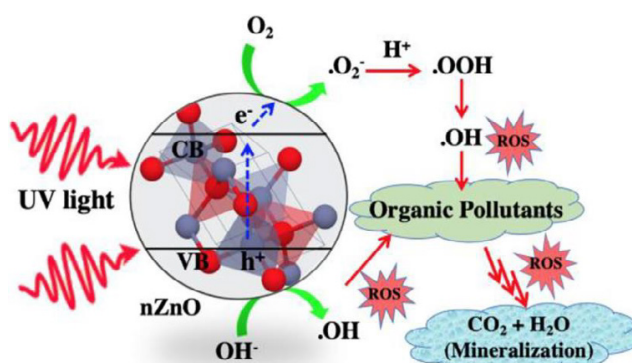


Fig. 7. Suggested scheme for the photo catalytic degradation of AR 114 by ZnO/Bentonite nanoparticles.

The size of Bentonite cavities is less than one nanometer. Also, SEM images showed that the morphology of the zeolite surface had changed after supporting ZnO on Bentonite. These results confirm the change in the surface morphology of the catalyst and the coverage of the zeolite surface with ZnO catalyst.

In SEM images taken from the catalyst, it is well presented that ZnO particles are placed and stabilized on the crystalline parts of zeolite Bentonite.

The SEM of Bentonite (Fig.4 A) displays the usual layered structure with numerous nanosized flakes of clay atoms with a sheet-like morphology. After precipitation method, the structure of Bentonite remained fixed and only the space between flakes was improved considerably.

FTIR spectra analysis

The molecular structure characteristics of the synthesized catalyst were identified by

FTIR spectra. The infrared spectrum of ZnO/Bentonite is measured by Perkin-Elmer FT-IR spectrophotometer with KBr pellets and illustrated in Fig 6. The FT-IR spectra of ZnO and ZnO/Bentonite in the range of 400–4000 cm⁻¹ were plotted. The bond in 450-500 cm⁻¹ represents to Zinc Oxide bond. The peak at 3450 cm⁻¹ corresponds to the tensile vibration of the hydroxyl group and the peak at 476 cm⁻¹ is originated from Zn–O stretch. The peak at 1660 cm⁻¹ represent to O-H bond of absorbed water molecules. In the catalyst doped on Bentonite, the absorption at 3700 cm⁻¹ is related to stretching vibration of OH group. After modification with Bentonite peaks appeared at 523 cm⁻¹ (Si–O–Mg(Fe)), 469 cm⁻¹ (Si–O–Al), and a strong peak at 1058 cm⁻¹ represent for Si-O stretching [21].

The nanophoto catalytic Mechanism

The photo catalytic degradation of AR 114 on ZnO/BT can be showed in Fig.7. The mechanism is

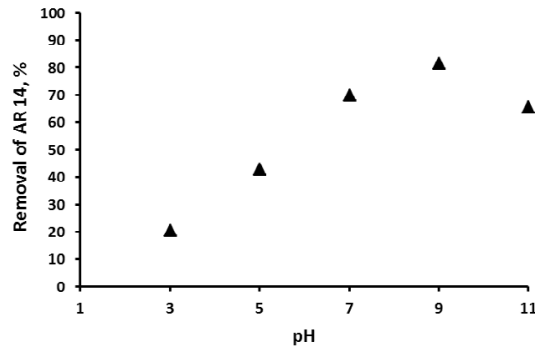
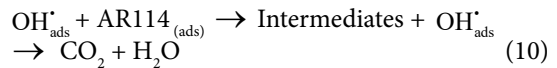
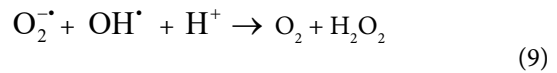
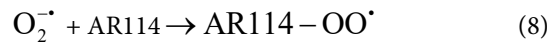
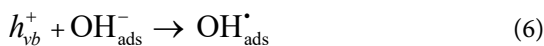
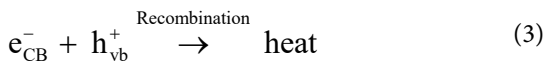
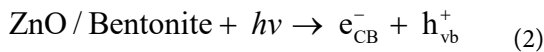


Fig. 8. The influence of pH on photo catalytic degradation of AR 114 (Initial concentration of AR114 at 20 mg/l, temperature at 25, and 120 min of reaction, and at 1.5 g/l of catalyst).

offered based on $\cdot\text{OH}$ generation studies and band gap analysis as reported by the previous reports [22]. The ZnO with a band gap energy of is 3.37 eV, is an n-type semiconductor with two electronic band structure including valence (VB) band and conduction band (CB). The transfer of an electron in the nano photo catalyst generates a positive hole on VB and subsequently several photochemical reactions occurred concurrently in the presence of water and oxygen on the catalyst surface. These mentioned holes on the VB oxidize the pollutants or inorganic species such as H_2O and hydroxyl ions to form hydroxyl radicals. The photo excited electron on the CB can reduce oxygen to produce different intermediate oxidant including $\text{HO}_2\cdot$, $\text{O}_2\cdot^-$, and $\text{OH}\cdot$. These intermediates have a short lifetime and very reactive, which accelerate groups of oxidation reactions result in the continuing degradation of contaminants to form CO_2 and H_2O . So, the production of reactive oxygen species is essential for the photo catalytic performance of ZnO. But, the recombination of the electron pairs and photo-generated holes can result in the short catalytic activity and photo thermal heat production (Eqs.2-10) [23].



Effect of pH on photo catalytic degradation of AR 114

To investigate the effect of pH on degradation of AR 114 in photo catalytic process, a solution with a concentration of 20 mg/l of the dye in the presence of catalyst was tested. At that time the pH of each sample was adjusted then the solutions were irradiated with ultraviolet light for 120 minutes. During this time, the samples were withdrawn at 20 minute intervals and their adsorption was measured by a spectrophotometer and the concentration of AR114 was determined. From Fig.8 it was clear that the degradation efficiency was increased with an increase in pH from 4 to 9 and then decreased at the pH of 11. This phenomenon can be because the zero points of charge (ZPC) of the ZnO/BT was 9, and below and above this pH the surface of catalyst was positively and negatively charged, respectively. And at the pH of ZPC, the surface of catalyst was neutral [24]. According to the mentioned reactions (Eqs.2-10), with an increase in pH the number of hydroxide ions and subsequently hydroxyl radicals were increased so the removal of AR 114 was increased, but further increase in pH results in the production of high hydroxyl radicals that the scavenging of them and lowering their numbers

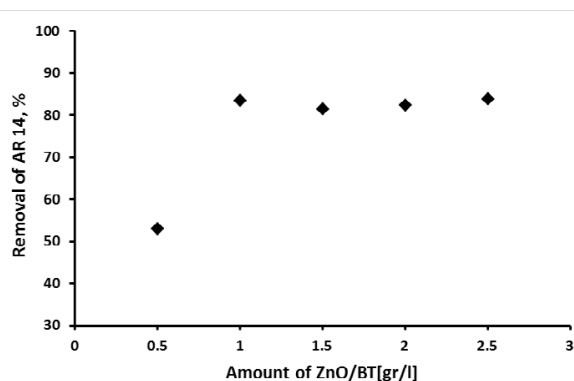


Fig. 9. The influence of catalyst concentration in degradation of AR 114 (pH at 9, Initial concentration of AR114 at 20 mg/l, the temperature at 25, and 120 min of reaction).

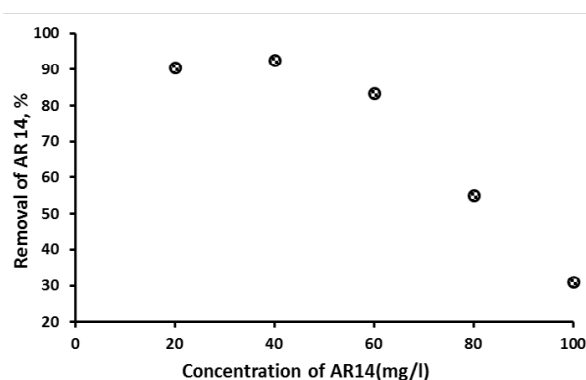


Fig. 10. The influence of initial concentration of AR114 on color removal efficiency (pH at 9, temperature at 25, and 120 min of reaction, at 1 g/l of catalyst).

happen, therefore the degradation of AR114 was decreased at pH of 11. The efficiency of photo catalytic process was increased with an increase in pH from 4 to 9 and then decreased with further increase in pH, because the molecules of AR114 has SO_3 group in its structure, and this group has negative charge in very high pH (pH=11), because of the repulsion with catalyst surface.

Influence of supported catalyst amount

In this section, different amounts of catalyst were added so that the catalyst concentration varied between 0.5 and 2.5 g/l, then the solutions were affected by the ultraviolet radiation. After starting reaction, the samples were withdrawn at 20-minute intervals and their absorption was measured by spectrophotometer at the maximum wavelength. The results in Fig. 9 showed that the color removal efficiency was increased with increase in catalyst concentration to 1 g/l, and then it was decreased with further increase in catalyst amounts. The reason is that by increasing the amount of photo

catalyst the number of active sites was increased, but more increase in catalyst mounts can lead to decrease in color removal efficiency because the light scattering occurred due to the collision of light with catalyst particles in the solution and a number of photons lost their energy. Therefore the rate of photo catalytic reactions decreased [25]. Above 1 g/l of catalyst the efficiency of the process was not increased considerably, therefore 1 g/l of nano catalyst was chosen as an optimum amounts from economic point of view.

The effect of initial concentration of AR114

The initial concentration of the dye was also considered as another very important parameter. Initial concentrations ranged from 20 to 50 mg/l under optimal experimental conditions were examined. The withdrawn samples were centrifuged to separate the catalyst particles; the absorption of the samples was measured by a spectrophotometer. According to Fig. 10, the removal efficiency of AR114 was increased with

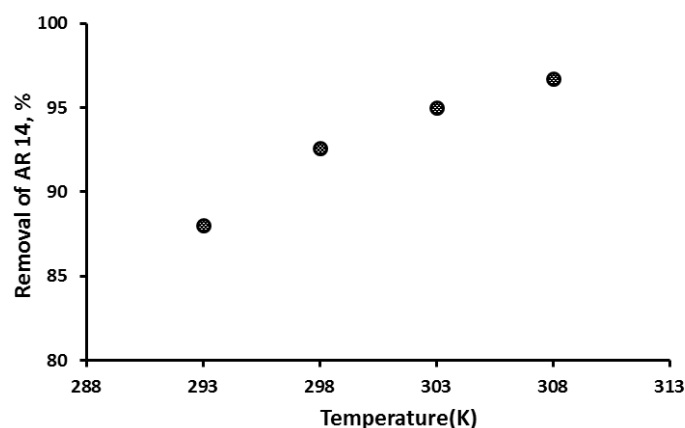


Fig. 11. Effect of temperature on the removal of AR114(pH at 9, Initial concentration of AR114 at 30 mg/l, and 120 min of reaction, at 1 g/l of catalyst)..

decrease in the concentration of AR114, and the reason for this is that as the color concentration increases, the absorption of ultraviolet light by the color molecules increases, and adequate photons do not contain adequate energy, so the conversion rate decreases with increasing color concentration. But at very low concentrations, the removal efficiency was reduced to some extent because the ratio of color molecules to the produced hydroxyl radicals was reduced and therefore radical scavenging can happen and subsequently the color removal efficiency reduced [26].

The influence of temperature

To investigate the effect of temperature on the photo catalytic removal of AR114, the temperature inside the reactor was controlled by thermostat.

The results in Fig. 11 showed the positive effect of temperature on color decomposition. The increase in temperature from 25 °C to 35 °C indicates that the color removal was increased. It should be noted that the reason that the temperature was not chosen exceed 35 °C was that at higher temperatures the probability of evaporation of the solution increased and caused the color concentration to change due to solvent evaporation. Since with increasing temperature, the transfer of electrons from the conduction band to Valance band in ZnO/Bentonite has been performed more rapidly, so the number of active sites in the catalyst was increased, thus degradation of AR 114 increased. So the optimum temperature was chosen at 35 °C .

The effect of ZnO before and after supporting Bentonite

As it can be seen from Fig. 12, the photo catalytic activity of ZnO was increased after inserting on Bentonite due to the increases in the contact surface between pollutant and photo catalytic molecules. The AR114 removal percentage in the presence of UV, UV/ZnO and UV/ZnO/Bentonite were about 26.5, 55% and 92.5% at two hours of reaction, respectively. The efficiency of stabilized photo catalytic was noticeable. The reason can be described by this fact that the two phenomena have played a major role in the photo catalysis including the adsorption of pollutants molecules on the surface of catalysts by forming electron–holes mechanism and subsequently the reaction of adsorbed pollutants with the produced hydroxyl radicals. The ZnO/bentonite Nano catalyst was synthesized with sol-gel method by Xu et al. In their study, about 90% of yellow acid 11 was degraded by ZnO/bentonite nanocatalyst under UV irradiation at 90 min of reaction [27], and the results are in agreement with present work.

CONCLUSION

In this research, the co-precipitation method was used to prepare the ZnO /Bentonit and results showed that it is a suitable and efficient technique. The synthesized catalyst was characterized by FT IR, XRD, and SEM techniques. Based on the experimental results, the efficiency of supported photo catalytic was improved significantly. The reason can be described by this fact that the two

phenomena have played a major role in the photo catalysis including the adsorption of pollutants molecules on the surface of catalysts by forming electron–holes mechanism and subsequently the reaction of adsorbed pollutants with the produced hydroxyl radicals. The efficiency of photo catalytic process was increased with increase in pH from 4 to 9 and then decreased with further increase in pH. The increase in temperature was enhanced the color removal efficiency. By increasing the amount of the stabilized photo catalyst, the efficiency was increased to some extent but beyond the optimum concentration of catalyst, the color removal efficiency was not significant.

The optimum conditions were achieved at 1g/l of catalyst, 30 mg/l of AR 114, pH at 9 and temperature at 35 °C. The AR114 removal percentage in the presence of UV, UV/ZnO and UV/ZnO/Bentonite were about 26.5, 55% and 92.5% after two hours of reaction, respectively.

ACKNOWLEDGEMENT

The authors wish to thank Sabzavar University of Medical Science, Sabzavar, Iran for financial support of this project.

CONFLICT OF INTEREST

The authors declare that there is no conflict of interest regarding the publication of this manuscript.

REFERENCES

- [1] A Garg, G Kaur, V K. Sangal, P K. Bajpai, S Upadhyay, *Environ. Eng. Res.* 25(5): 753(2020). <https://doi.org/10.4491/eer.2019.246>.
- [2] M. Saghi , A. Shokri, A. Arastehnodeh, M.Khazaeinejad, A. Nozari , *J. Nanoanalysis.*, 5, 163(2018).
- [3] A. Shokri, K. Mahanpoor, M. Nasiri Shoja, *Bulg. Chem. Communications*, 50, 27 (2018).
- [4] A. Shokri, *Archives of hygiene science*, 5(4), 229(2016).
- [5] A. Shokri, *Iran J chem. Chem. Eng. Iran. J. Chem. Chem. Eng.* 38 (2), 113(2018).
- [6] A. Shokri, M. Salimi, T. Abmatin, *Fresen Environ Bull.*, 26, 1560(2017).
- [7] A. Shokri, A. H. Joshaghani, *Russ. J Appl Chem.*, 89, 1985(2016). <https://doi.org/10.1134/S1070427216120090>
- [8] Barbosa, L.V., et al., *Catal Today*, 246, 133(2015). <https://doi.org/10.1016/j.cattod.2014.09.019>
- [9] A. Shokri, *J Nano Dimens* 7, 160 (2016). <https://doi.org/10.7508/ijnd.2016.02.008>.
- [10] Bel Hadjtaief, H., et al., H. B. Hadjtaief, S. B. Ameur, P.D. Costa, M.B. Zina, M.E. Galvez, *Appl Clay Science*, 152: 148(2018). <https://doi.org/10.1016/j.clay.2017.11.008>
- [11] H. Pouraboulghasem, M. Ghorbanpoor, R. Shayegh, S. Lotfiman, *J Central South University*, 23(4): 787(2016). <https://doi.org/10.1007/s11771-016-3124-y>
- [12] S. Lotfiman, and M. Ghorbanpour, *Surface and Coatings Technol*, 310,129(2017). <https://doi.org/10.1016/j.surfcoat.2016.12.032>
- [13] S. Gilani, M. Ghorbanpour, and A. Parchehbaf Jadid, *J Nanostructure in Chem* , 6(2): 183(2016). <https://doi.org/10.1007/s40097-016-0194-1>
- [14] M. Akkari, P. Aranda, H. Ben Rhaiem, A. Ben Haj Amara, E. Ruiz-Hitzky, *Appl Clay Sci*, 131: 131(2016). <https://doi.org/10.1016/j.clay.2015.12.013>
- [15] K. Karthik, S. Dhanuskodi, C. Gobinath, S. Sivaramkrishnan, *Spectrochim. Acta, Part A* 139, 7(2015). <https://doi.org/10.1016/j.saa.2014.11.079>
- [16] Q. Luo, X. Yu, B. Lei, H. Chen, D. Kuang, C. Su, *J. Phys. Chem. C* 116, 8111(2012). <https://doi.org/10.1021/jp2113329>.
- [17] D. Barpuzary, M. Qureshi, *Appl. Mater. Interfaces* 5, 11673(2013). <https://doi.org/10.1021/am403268w>
- [18] J. Gajendiran, V. Rajendran, *Mater. Lett.* 116, 311(2014). <https://doi.org/10.1016/j.matlet.2013.11.063>
- [19] A Ī Vaizogullar, *J. Mex. Chem. Soc* 62,1(2018) <http://dx.doi.org/10.29356/jmcs.v62i1.578>
- [20] R. KR, K. KV, B. Prasad SB, S. SK, J. HM, *Polyhedron* 120,169(2016). <https://doi.org/10.1016/j.poly.2016.08.029>
- [21] T Chakraborty, A Chakraborty, M. Shukla & Tanmay Chattopadhyay: *J Coordination Chem.*, (2019) <https://doi.org/10.1080/00958972.2018.1560429>
- [22] A.M. Abdullah, M.Á. Gracia-Pinilla, S.C. Pillai, K. O'Shea, *Molecules* 24 (11), 2147(2019). <https://doi.org/10.3390/molecules24112147>.
- [23] K. A. Sultana, M.d. Tariqul Islamb, J. A. Silva, R. S. Turley, J. A. Hernandez-Viezas, J. L. Gardea-Torresdey, J. C. Noveron, *J Molecular Liquids*, 307, 2020. <https://doi.org/10.1016/j.molliq.2020.112931>
- [24] A. Shokri, K. Mahanpoor, D. Soodbar, *J Environ Chem Eng* 4, 585(2016). <https://doi.org/10.1016/j.jece.2015.11.007>
- [25] A. Shokri, K. Mahanpoor, D.Soodbar, *Fresen. Environ. Bull.* 25, 500(2016).
- [26] T R. Waghmode, M B. Kurade, R T. Sapkald, C H. Bhosale, B Hun Jeon, S P. Govindwar, *J Hazard Matter* 371,115(2019). <https://doi.org/10.1016/j.jhazmat.2019.03.004>
- [27] H. Xu, T. Yu, J. Liu, *Mater. Lett.*, 117, 263(2014). <https://doi.org/10.1016/j.matlet.2013.12.022>